Bayesian inference of cardiac models emulated with a time series Gaussian process

Yuzhang Ge[1], Dirk Husmeier[1], Alan Lazarus [1], Arash Rabbani[2], Hao Gao[1]
[1]School of Mathematics and Statistics, University of Glasgow
Glasgow G12 8SQ, UK
Emails: 2670035g@student.gla.ac.uk; Dirk.Husmeier@glasgow.ac.uk;
Alan.Lazarus@glasgow.ac.uk; Hao.Gao@glasgow.ac.uk
[2]School of Computing/University of Leeds
Leeds LS2 9JT, UK
Emails: A.Rabbani@leeds.ac.uk

Abstract - The objective of this research is to estimate the specific biophysical parameters of a cardiac mechanics model using a time series of variables that can be acquired in the clinic. This method is driven by the need to infer the passive stiffness of the myocardium to diagnose cardiophysiological diseases, which requires the measurement of the volume of the left ventricle (LV) of the heart at different time points. Although there have been many advancements in cardiac models, their computation is complex and costly. To overcome this challenge, we propose a method that utilizes a Gaussian process to construct a statistical model for emulation. Since the LV volumes are acquired in a time series, we employ the Kronecker product to compute two covariance matrices separately for time and biophysical parameters. Once we construct an accurate emulator to represent the passive filling process of the cardiac mechanics model during diastole, we can estimate the biophysical parameters inversely. We also aim to evaluate the impact of increasing the number of time points on reducing the uncertainty of the inverse estimation in this study.

Keywords: Gaussian process; Time series kernel; Inverse estimate; Cardiac model

1. Introduction

The field of cardio-mechanics modelling has made impressive progress in recent years, with mathematical models being used to predict various quantities of interest (QoIs) related to the biophysical structure of the cardiovascular system [1]. However, determining the biophysical parameters of these models can be challenging, particularly because different patients have different sets of parameters that can affect the QoIs. One common approach to inferring these parameters is via iterative optimization, where we define a loss function that compares model predictions and measured QoIs and optimize this function to obtain our set of parameter estimates. Typically, this method requires running thousands of simulations of the mathematical model, which compounds the computational costs associated with the underlying mathematical model.

In this study, we focus on the cardio-mechanics of the left ventricle of the human heart in diastole, which is dependent on unknown passive properties of the myocardium that can only be inversely inferred for real patients using in vivo measurements, i.e. magnetic resonance imaging (MRI) scans [1] To reduce the computational burden of inferring biophysical parameters, we use a method called emulation [2, 3], which involves creating an approximate model, or emulator, that can accurately predict the QoIs generated by the mathematical model for different sets of biophysical parameters [4].

Previous work in this area has focused on using QoIs from MRI scans at fixed time points (specifically, end-diastole) [5]. However, in this study, we use a time series of QoIs as the input to the emulator. To do this, we use an upgraded version of the Gaussian process (GP) model developed by Roberts, S. et al. [6], which allows us to model the relationship between time, biophysical parameters, and the QoIs. Once we have trained our emulator, we use it to estimate the unknown myocardial parameters based on a time series of observed QoIs extracted from MRI scans. This process is known as inverse estimation, and we use Bayesian inference to estimate the distribution of different biophysical parameters. By sampling from this distribution, we can quantify the uncertainty in our inference.
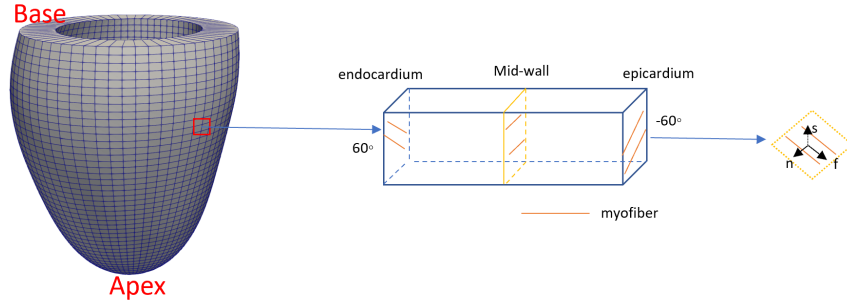
Fig. 1: The left part is the LV mesh with 5600 nodes and 13600 elements, the middle is a schematic illustration of myofibre (myocyte) rotation from endocardium to epicardium, and the right is a local f-s-n material coordinate system.

2. Methodology

2.1. The cardiac model

A previously developed cardiac mechanic model of the left ventricle (LV) of the heart is adopted in this study [7], shown in Figure 1. In brief, the reference LV geometry was derived from a healthy volunteer at early diastole. In diastole, the LV is passively expanded with increased diastolic pressure until the end of diastole. Note during diastole, there is no active contraction. The remainder of this section summarises the mathematical details. For background reading, we refer the reader to [8].

Myocardial passive mechanical property plays a significant role in LV dynamics in diastole, and has been usually characterized by some strain energy functions. Here, we model the myocardium using the so-called Holzapfel-Ogden constitutive law (H-O) [9], which further takes into account the layered myofibre architecture of the myocardium, denoted as the fibre-sheet-normal system ($\mathbf{f} - \mathbf{s} - \mathbf{n}$) as shown in figure 1, the right panel. The H-O law is

$$W = \frac{a}{2b}e^{b(I_1-3)} + \sum_{i=\mathrm{f,s}} \frac{a_i}{2b_i}\left[e^{b_i(I_{4i}-1)^2} - 1\right] + \frac{a_{\mathrm{fs}}}{2b_{\mathrm{fs}}}\left[e^{b_{\mathrm{fs}}I_{8fs}} - 1\right], \tag{1}$$

where a, b are the parameters related to the extracellular matrix response, a_f, b_f are the material parameters along the myofibre direction ($\mathbf{f}$), a_s and b_s are related to the sheet fibre ($\mathbf{s}$) contribution, finally a_fs and b_fs are the shear effect in the sheet-fibre ($\mathbf{f} - \mathbf{s}$) plane. The strain invariant $I_1 = \mathrm{tr}(\mathbf{C})$ with $\mathbf{C} = \mathbf{F}^\mathrm{T}\mathbf{F}$ the right Cauchy-Green tensor, and $\mathbf{F}$ is the deformation gradient. The invariants $I_{4\mathrm{f}} = \mathbf{f}_0 \cdot (\mathbf{C}\mathbf{f}_0)$ and $I_{4\mathrm{s}} = \mathbf{s}_0 \cdot (\mathbf{C}\mathbf{s}_0)$ represent stretch-related invariants along the myofibre and sheet directions, in which $\mathbf{f}_0$ and $\mathbf{s}_0$ are the myofibre and sheet directions in the reference configuration. The mechanical coupling between the myofibre and sheet is represented by $I_{8\mathrm{fs}} = \mathbf{f}_0 \cdot (\mathbf{C}\mathbf{s}_0)$ reflects.

From Equation (1), the Cauchy stress of the myocardium ($\boldsymbol{\sigma}$) can be derived as $\boldsymbol{\sigma} = \frac{1}{\det \mathbf{F}}\mathbf{F}\left(\frac{\partial W}{\partial \mathbf{F}}\right) - p\mathbf{I}$, where p is the Lagrange multiplier to enforce the incompressibility. The boundary value problem for the LV dynamics in diastole in the current configuration can be written as

$$\left.\begin{array}{ll} \nabla \cdot \boldsymbol{\sigma} + \boldsymbol{b} = 0 & \text{in } \Omega \\ \boldsymbol{\sigma} \cdot \mathbf{n} = \mathbf{t} & \text{in } \Gamma^\mathrm{N} \\ \mathbf{u} = \mathbf{u}_0 & \text{in } \Gamma^\mathrm{D}, \end{array}\right\} \tag{2}$$

where $\mathbf{b}$ is the body force density per unit volume, $\mathbf{u}$ is the displacement field, $\mathbf{n}$ is the normal direction of LV surface (Γ^N), $\mathbf{t}$ is the traction force resulting from the LV cavity pressure, $\mathbf{u}_0$ is the prescribed displacement at the Dirichlet boundary Γ^D, and Γ^N is the Neumann boundary. A pressure profile that linearly increases from 0 to the end-diastolic blood pressure (EDP) in millimetres of mercury (mmHg) is imposed on the endocardial surface of the left ventricle. The basal plane is constrained in both the longitudinal and circumferential directions but is allowed to expand radially as shown in figure 1. The system of equations (Equation (2)) can only be solved numerically for a patient LV geometry by using the general-purpose finite-element

package ABAQUS [1]. We note that one simulation using ABAQUS can take up to 5 mins on a Linux workstation without parallel computing (Intel Xeon Gold 6138 2.0GHz, 128GB memory).

2.2. Time-series Gaussian process

To deal with the high computational costs of numerical simulations from the original cardiac mechanics model, we follow [4] and build an emulator. The objective of [4] was to predict various QoIs (LV cavity volume and circumferential strains) at the end of diastole during the heart's pump cycle as a function of the biophysical parameters associated with the H-O law. The biophysical parameters can then be estimated based on a comparison between predicted QoIs and their counterparts extracted from a patient's MRI scan at end-diastole. Our present work focuses on only one of the QoIs considered in [4] – the left ventricular volume (LVV) at end-diastole – and takes a time series of different measurements between early and end-diastole, instead of a single time point. Focusing on only the LVV is motivated with clinical applications in mind, as this quantity can be extracted from MRI scans automatically using recent advances in machine learning [10]. Our approach is naturally formulated as an emulator of a scalar quantity (the LVV) defined over a Cartesian product space of biophysical parameters $\mathbf{X}$ and time $\mathbf{T}$.

Consider $\mathbf{X} = [\mathbf{x}_1, \mathbf{x}_2....\mathbf{x}_n]$, where $\mathbf{x}_i$ is the input variable for the ith case, and the output space

$$\mathbf{Y} = [\mathbf{f}(\mathbf{x}_1)....\mathbf{f}(\mathbf{x}_n)] \tag{3}$$

with

$$\mathbf{f}(\mathbf{x}_i) = [f(\mathbf{x}_i, t_1), \ldots, f(\mathbf{x}_i, t_e)] \tag{4}$$

a time series of LV volumes in diastole as our QoI, where $\mathbf{f}$ has a joint Gaussian distribution [6]: $\mathbf{Y} \sim \mathcal{N}(\boldsymbol{\mu}, \mathbf{K})$, where $\boldsymbol{\mu}$ is the mean of $\mathbf{Y}$, and $\mathbf{K}$ is the covariance matrix with $i, j \in [1, ..., n]$. For m unobserved cases $\mathbf{X}^* = [\mathbf{x}_1^*, ..., \mathbf{x}_m^*]$, we also assume $\mathbf{f}(\mathbf{X}^*) \sim \mathcal{N}(\boldsymbol{\mu}^*, \sigma^{2*})$, then we have

$$\boldsymbol{\mu}^* = \mathbf{K}(\mathbf{X}, \mathbf{X}^*)^T \mathbf{K}(\mathbf{X}, \mathbf{X})^{-1} \mathbf{Y} \tag{5}$$

$$\sigma^{*2} = \mathbf{K}(\mathbf{X}^*, \mathbf{X}^*) - \mathbf{K}(\mathbf{X}, \mathbf{X}^*)^T \mathbf{K}(\mathbf{X}, \mathbf{X})^{-1} \mathbf{K}(\mathbf{X}, \mathbf{X}^*), \tag{6}$$

in which σ^{*2} is the covariance of $\mathbf{f}(\mathbf{X}^*)$ [3]. Now we follow [6] and consider a time-series GP, where the outputs are defined over the Cartesian product space of the biophysical parameters $\mathbf{X} = [\mathbf{x}_1, \mathbf{x}_2....\mathbf{x}_n]$, where each $\mathbf{x}_i$ represents a k-dimensional biophysical parameter vector, and time, $\mathbf{T} = (t_1, \ldots, t_e)$. To reduce the computational complexity of a general GP, we make the following Kronecker product assumption:

$$cov(\mathbf{Y}, \mathbf{Y}) = \mathbf{K}_1(\mathbf{X}, \mathbf{X}) \otimes \mathbf{K}_2(\mathbf{T}, \mathbf{T}) \tag{7}$$

$$= \begin{pmatrix} k_1(\mathbf{x}_1, \mathbf{x}_1) \times \mathbf{K}_2(\mathbf{T}, \mathbf{T}) & \cdots & k_1(\mathbf{x}_1, \mathbf{x}_n) \times \mathbf{K}_2(\mathbf{T}, \mathbf{T}) \\ \vdots & \ddots & \vdots \\ k_1(\mathbf{x}_n, \mathbf{x}_1) \times \mathbf{K}_2(\mathbf{T}, \mathbf{T}) & \cdots & k_1(\mathbf{x}_n, \mathbf{x}_n) \times \mathbf{K}_2(\mathbf{T}, \mathbf{T}) \end{pmatrix}$$

$$= \begin{pmatrix} k_1(\mathbf{x}_1, \mathbf{x}_1) \cdot k_2(t_1, t_1) & \cdots & k_1(\mathbf{x}_1, \mathbf{x}_n) \cdot k_2(t_1, t_e) \\ \vdots & \ddots & \vdots \\ k_1(\mathbf{x}_n, \mathbf{x}_1) \cdot k_2(t_e, t_1) & \cdots & k_1(\mathbf{x}_n, \mathbf{x}_n) \cdot k_2(t_e, t_e) \end{pmatrix}$$

The kernel function for parameter $\mathbf{X}$ is $k_1(\cdot)$, and the kernel function for time is $k_2(\cdot)$. The Kronecker product offers several advantages, including the ability to separate the parameter space and the temporal space. This allows separate kernels to calculate the mean function and the splitting of a large covariance matrix into two smaller matrices, resulting in significant reductions in computational cost [6], specifically,

$$[cov(\mathbf{Y}, \mathbf{Y})]^{-1} = \mathbf{K}_1^{-1}(\mathbf{X}, \mathbf{X}) \otimes \mathbf{K}_2^{-1}(\mathbf{T}, \mathbf{T}) \tag{8}$$

This reduces the computational complexity from $O((ne)^3)$ to $O(n^3 + e^3)$.

3. Results

3.1. Training set generation

Our aim is to apply the time-series GP described in the previous section to emulate the time-series LVV in diastole as a function of myocardial passive parameters. In the present work, we only consider two of the parameters of the H-O law (1): $[a, b]$, with prior supports $a \in [0.1, 5.0]$ and $b \in [0.1, 5.0]$. All other material parameters have been fixed. The motivation for this is to avoid identifiability problems, as discussed in [5] and [11]. Put differently, our study is intended to be a proof of concept study for the LVV time-series emulator, and for that reason, we have eliminated confounding factors related to a potential intrinsic lack of biophysical parameter identifiability. Hence, our parameter space is $\mathbf{X} = [a, b]$, and the emulated QoI is the LVV for different numbers of time points $\mathbf{T} = [t_1, .., t_e]$ during diastole. In the present study, we have set $e = 1$, $e = 2$, and $e = 10$. Note that $e = 1$ is the limiting case considered in [5] where only a single time point at end-diastole is available. For $e = 2$ we include two time points: one at mid-diastole and one at end-diastole. Finally, $e = 10$ corresponds to a time series of 10 equidistant measurements between early and end-diastole. Note that our "measurements" are LVVs, and application of this methodology in the clinic would require the measurement of $e = 10$ LVVs from MRI scans. We then aim to quantify the improvement in parameter estimation accuracy as a consequence of longer time series, i.e. larger values of e, to help decide if this justifies the higher efforts in terms of medical image processing.

For building the emulator, we have covered the biomechanical parameter space with a space-filling design using a Sobol sequence. Sobol sequences have been found to be effective in generating random samples in high-dimensional spaces, especially in situations where evenly distributed points are crucial and rapid convergence is desirable [12]. We have covered the space with 2000 points in total, using 1900 as a training set for training the emulator and using an independent set of 100 points for testing the accuracy of biophysical parameter inference, as shown in figure 2 (a).

3.2. Time-series GP

For the Gaussian process, we chose a squared exponential ARD kernel [13] for $\mathbf{K}_1(\mathbf{X}, \mathbf{X})$, i.e. the covariance matrix in biophysical parameter space, and a kernel from the Matèrn family for $\mathbf{K}_2(\mathbf{T}, \mathbf{T})$, i.e. the covariance matrix in the temporal domain. The motivation for the latter choice is to explore different degrees of smoothness, as shown in Table 1. In our simulation studies, we found that the Matèrn 3/2 kernel gave the highest adjusted R^2 score and the least mean squared error (MSE) for the 100 test cases. We, therefore, used the Matèrn 3/2 kernel in the following analysis. Figure 2(a) shows the prediction using the trained time-series GP for one test case, and figure 2(b) for all tests. It can be seen that this time-series GP can well emulate the time-series LVV in diastole with negligible differences compared to the simulated data.

Table 1: The choice of the kernel function $k_2(\cdot)$ when applied to the 100 test cases.

Kernel function	R^2 score	MSE
k_2=Matèrn 5/2	0.9993	0.022
k_2=Matèrn 3/2	0.9996	0.021
k_2=k_1	0.9962	0.030

3.3. Inverse problem

Ideally, we would assess the performance of our model using real data measured from MRI scans. However, this introduces several complications, such as model discrepancy [14] and a lack of knowledge of the ground truth parameter set. For this reason, we instead chose to construct a synthetic data study, where the ground truth parameters are known. This is done by simulating the signal, $\mu(\theta)$ (or LVV), from the cardio mechanical model described in Section 2.1 and corrupting these signals with Gaussian noise:

$$\tilde{\mathbf{y}} = f(\theta) + \epsilon, \epsilon \sim \mathcal{N}(0, \sigma_m^2) \tag{9}$$
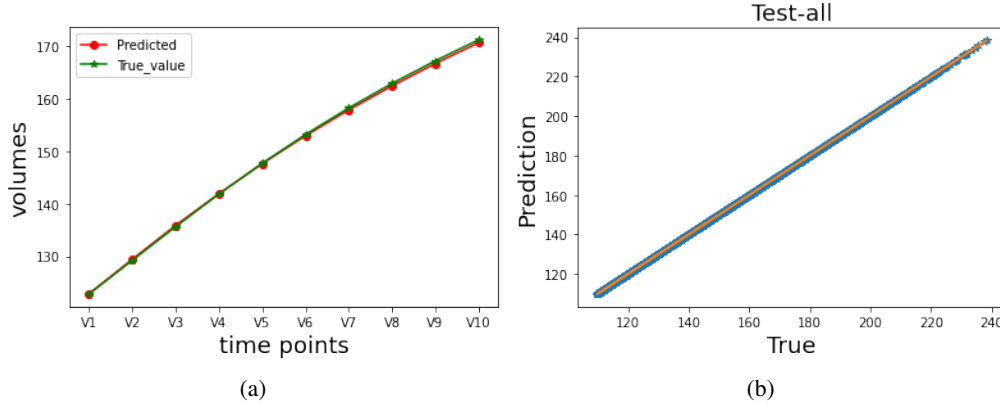
Fig. 2: (a) The predicted time-series LVV for one test case, and (b) for all test cases by using Matèrn 3/2 for k_2

with $\sigma_m^2 = 0.01$. Here $\boldsymbol{\theta} = [a, b]$ is a set of material parameters. We generated 20 synthetic test data points in this manner, each at a different combination of the material parameters a and b.

The prior of $\boldsymbol{\theta}$ is the uniform distribution ($\tilde{a} \sim U(0.1, 5.0)$ and $\tilde{b} \sim U(0.1, 5.0)$). The likelihood function can be defined as $\tilde{\mathbf{y}} \sim \mathcal{N}(\mathbf{f}(\boldsymbol{\theta}), \sigma_m^2)$, where the cardio-mechanical model $\mathbf{f}(\boldsymbol{\theta})$ is expensive to evaluate. For that reason, we replace this with the comparatively cheap time-series GP to evaluate emulator $\boldsymbol{\mu}(\boldsymbol{\theta})$ and assume that $\tilde{\mathbf{y}} \sim \mathcal{N}(\boldsymbol{\mu}(\boldsymbol{\theta}), \sigma_m^2)$. The negative log-likelihood is

$$-\log(p(\tilde{\mathbf{y}}|\boldsymbol{\mu}(\boldsymbol{\theta}))) = \frac{1}{2}\log(2\pi\sigma_m^2) + \frac{1}{2\sigma_m^2}\sum_{i=1}^{e}(\tilde{y}_i - \mu(\boldsymbol{\theta}, t_i))^2. \tag{10}$$

By using Bayesian inference, we can apply the No-U-Turn Sampler (NUTS) to take samples from the posterior $p(\boldsymbol{\theta}|\mu, \tilde{\mathbf{y}})$. NUTS is a powerful MCMC algorithm that adapts to the geometry of the target distribution and can explore complex and high-dimensional distributions more efficiently. There is no need to define the number of iterations since NUTS automatically sets its parameters, efficient sampling, lower sample correlation, and faster convergence [15].

Figure 3 shows the posterior distributions obtained from our MCMC simulations by applying a kernel density estimator to a set of 10,000 MCMC samples. Three test cases were chosen, one with both parameters in the middle of the parameter space, and the other two with one parameter near the lower bound and the other one near the upper bound. The figures show the marginal posterior distributions for the parameter a (left panel) and the parameter b (right panel), with the vertical bar showing the ground truth values. We can see that for $e = 10$, the posterior distributions peak around the true value, whereas for $e = 1$, the posterior distributions are diffuse, with substantial posterior probability mass leaking away from the true values.

Table 2: Comparing the variance of the posterior of figure 3.(a) and(b)

Num of time points	Variance of the posterior of a	Variance of the posterior of b
e=1	0.26	1.94
e=2	0.06	0.59
e=10	0.02	0.22

From table 2, we could find that the uncertainty of inference on the first case in figure 3 has a fourfold reduction by adding one more time point. After increasing the number of time points to 10, variances of the posterior distribution shrink to almost one-third of that with two-time points. Figure 3 shows parameter estimation results for two other test cases. The effect of applying more time points on reducing inference uncertainty is similar. Our study thus allows us to quantify the improvement
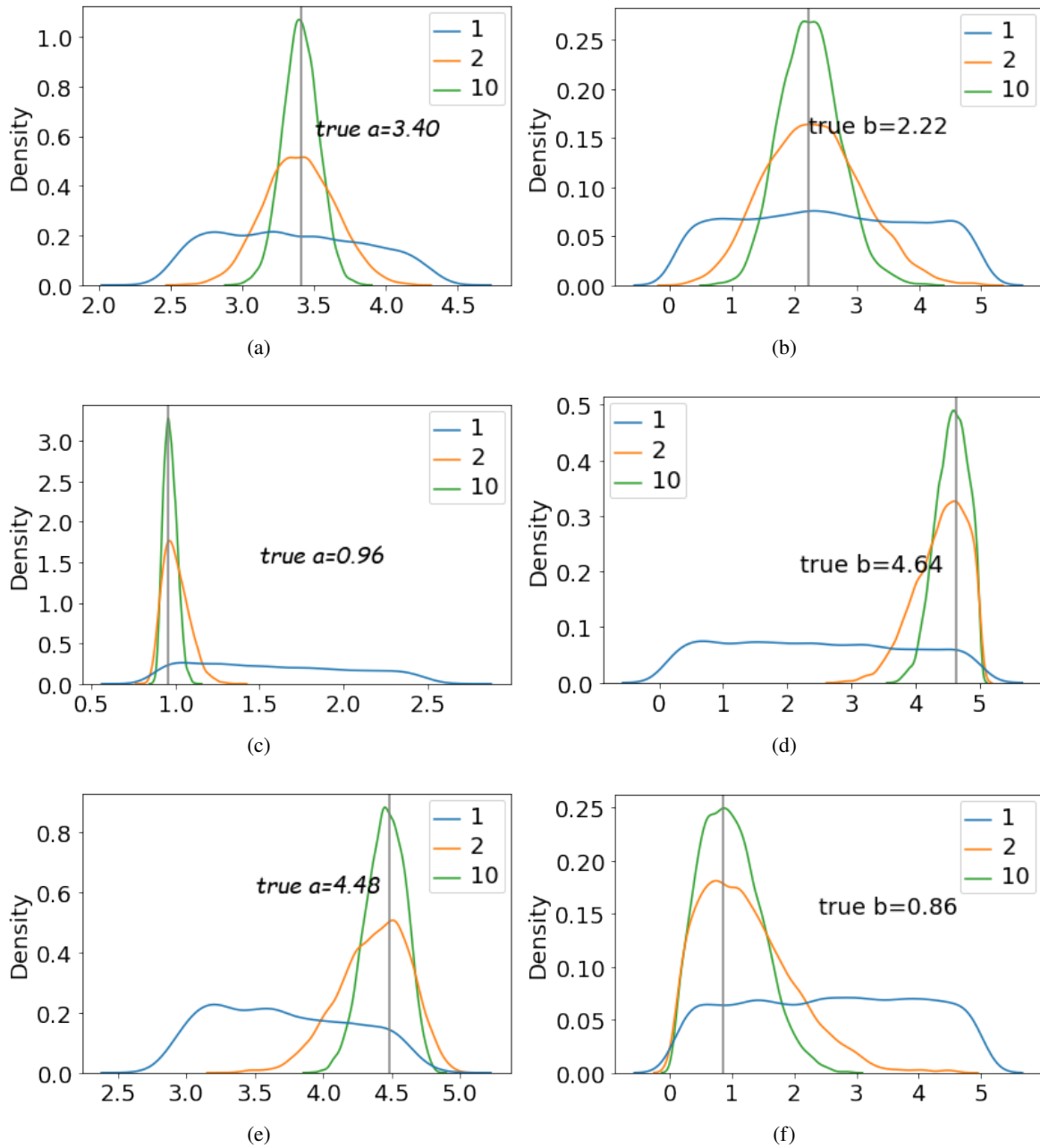
Fig. 3: Posterior distributions of three cases for *a* and *b* respectively.

in estimation accuracy and reduction in posterior uncertainty as a consequence of increasing the length of the time series. We emphasize again that in a clinical setting, this corresponds to increasing the number of LVV measurements from MRI scans.
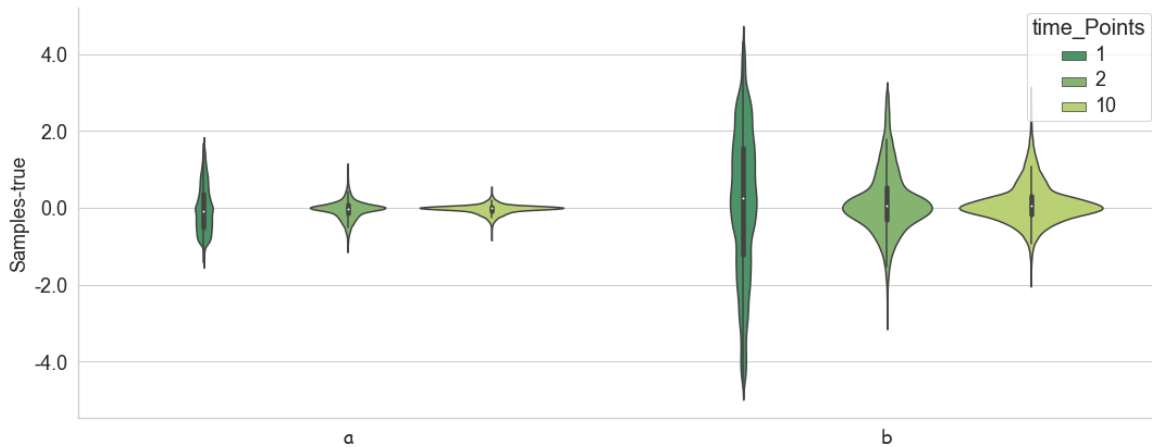
Fig. 4: Residual of 20 test cases for $e = 1$, $e = 2$ or $e = 10$ time points.

Figure 4 shows an alternative representation in terms of violin plots of the residuals, defined as the difference between samples and true values. After getting residuals for different numbers of time points e, all MCMC samples of the residuals of the 20 test cases were combined to quantify the reduction in the posterior uncertainty when increasing the number of time points e. This figure is consistent with the previous one for the three selected parameter sets, see figure 3.

4. Discussion

In the present paper, we have used a Gaussian process surrogate model with a Kronecker product decomposition of the covariance matrix into separate contributions from the biophysical parameters and the time series. The purpose of this emulator is to avoid the high computational costs of running simulations using the original cardiac model [1], as defined in Section 2.1. Our results suggest that our emulator accurately reproduced the LVV time series for different values of the passive parameters of the myocardium. In the process of inferring unknown material parameters, we have used the emulator to approximately sample parameters from the posterior distribution, by following [5] and running MCMC simulations on the emulated log-likelihood. Given the high computational costs of its numerical simulations, this process would be practically infeasible for the original cardiac mechanics model.

Despite the successful application of the surrogate model in this paper, there are limitations that currently prevent its application in the clinic. One limitation is that the emulator was built under the assumption of a fixed LV geometry. This does not allow for patient-specific variations, which will adversely affect the model predictions. To overcome this limitation, our surrogate model needs to be extended to include a low-dimensional representation of the LV geometry as an additional input to the emulator, in addition to the material parameters themselves, which can be done following the procedure described in [11].

The second challenge is to accurately extract the time series of LVV from MRI scans [10]. In our experiments, all LVVs were synthetically generated based on simulations from the cardiac model, which guarantees a higher degree of accuracy than might be available in real clinical applications. Thus, further research is needed to examine whether the LVV volumes from MRI scans can be used by the surrogate model to predict material parameters at a comparable level of accuracy as achieved in our simulation study.

Finally, our study has been restricted to inferring only two of the myocardial parameters, while keeping the remaining six parameters fixed. This has been partly motivated by the study in [5], which by carrying out a global sensitivity analysis has shown that not all parameters are relevant for the LVV, i.e. some parameters can be varied without affecting the LVV and are thus unidentifiable. This suggests that additional QoIs, in addition to the LVV, should be considered in future studies.

5. Conclusion

We have proposed a Gaussian process surrogate model defined over the Cartesian product space of time and biophysical parameters. We have modelled the full covariance matrix of the Gaussian process as a Kronecker product of two separate covariance matrices, one defined in the biophysical parameter space, the other defined over time. We have shown that this provides an efficient and accurate way of estimating the unknown material parameters of the cardiac mechanics model, with potential future clinical applications for improved diagnosis of cardiophysiological diseases. However, an additional hurdle to overcome is the integration of patient-specific characteristics of the left ventricle geometry into the proposed emulation framework. This will be based on the dimension reduction approach proposed in [11] and is the subject of our future work.

References

[1] H. Gao, K. Mangion, D. Carrick, D. Husmeier, X. Luo, and C. Berry, "Estimating prognosis in patients with acute myocardial infarction using personalized computational heart models," *Scientific reports*, 2017.

[2] S. Conti, J. P. Gosling, J. E. Oakley, and A. O'Hagan, "Gaussian process emulation of dynamic computer codes," *Biometrika*, 06 2009.

[3] R. B. Gramacy, *SURROGATES : Gaussian process modeling, design, and optimization for the applied sciences.* Routledge, 2021.

[4] V. Davies, U. Noè, A. Lazarus, H. Gao, B. Macdonald, C. Berry, X. Luo, and D. Husmeier, "Fast parameter inference in a biomechanical model of the left ventricle by using statistical emulation," *Journal of the Royal Statistical Society. Series C, Applied Statistics*, vol. 68, no. 5, p. 1555, 2019.

[5] A. Lazarus, D. Dalton, D. Husmeier, and H. Gao, "Sensitivity analysis and inverse uncertainty quantification for the left ventricular passive mechanics," *BMMB*, 2022.

[6] S. Roberts, M. Osborne, and S. Aigrain, "Gaussian processes for time-series modelling," *Philosophical Transactions of the Royal Society A: Mathematical, Physical and Engineering Sciences*, 2013.

[7] H. Gao, W. Li, L. Cai, C. Berry, and X. Luo, "Parameter estimation in a holzapfel–ogden law for healthy myocardium," *Journal of engineering mathematics*, vol. 95, pp. 231–248, 2015.

[8] J. D. Humphrey, *Cardiovascular solid mechanics: cells, tissues, and organs.* Springer Science & Business Media, 2013.

[9] G. A. Holzapfel and R. W. Ogden, "Constitutive modelling of passive myocardium: a structurally based framework for material characterization," *Philosophical Transactions of the Royal Society A: Mathematical, Physical and Engineering Sciences*, vol. 367, pp. 3445–3475, 09 2009.

[10] R. Arash, G. Hao, A. Lazarus, D. Dalton, G. Yuzhang, M. Kenneth, B. Colin, and H. Dirk, "Image-based estimation of the left ventricular cavity volume using deep learning and gaussian process with cardio-mechanical applications," *Computerized Medical Imaging and Graphics*, 2023.

[11] A. Lazarus, H. Gao, X. Luo, and D. Husmeier, "Improving cardio-mechanic inference by combining in vivo strain data with ex vivo volume-pressure data," *Journal of the Royal Statistical Society: Series C (Applied Statistics)*, 2022.

[12] U. Noè, A. Lazarus, H. Gao, V. Davies, B. Macdonald, K. Mangion, C. Berry, X. Luo, and D. Husmeier, "Gaussian process emulation to accelerate parameter estimation in a mechanical model of the left ventricle: a critical step towards clinical end-user relevance," *Journal of the Royal Society Interface*, vol. 16, no. 156, p. 20190114, 2019.

[13] M. Seeger, "Gaussian processes for machine learning," *International journal of neural systems*, vol. 14, no. 02, pp. 69–106, 2004.

[14] A. Lazarus, *Surrogate modelling of a patient-specific mathematical model of the left ventricle in diastole.* PhD thesis, University of Glasgow, 2022.

[15] M. D. Hoffman, A. Gelman, *et al.*, "The no-u-turn sampler: adaptively setting path lengths in hamiltonian monte carlo.," *J. Mach. Learn. Res.*, vol. 15, no. 1, pp. 1593–1623, 2014.